A glimpse of gluons through deeply virtual Compton scattering

M. Defurne
On behalf of the DVCS Hall A collaboration

M. Defurne *et al.*, Nature Communications 8, 1408 (2017)

CEA Saclay - IRFU/SPhN

January 24^{th} 2018

The nucleon: a formidable lab for QCD

- The nucleon is a dynamical object made of quarks and gluons.
- This dynamics is ruled by the strong interaction.
- A perturbative approach from first principles to unravel this dynamics is impossible due to the large size of the strong coupling constant.

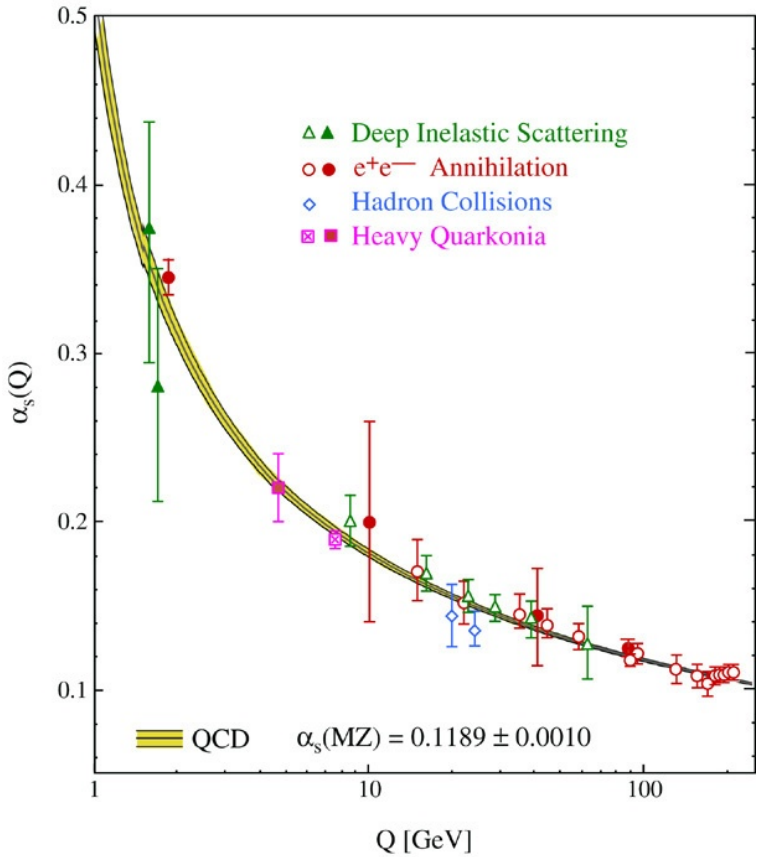

Although non-perturbative approaches (DSE, lattice QCD) starts making progress, the experimental approach remains more convenient to get complex information about this dynamics.

A set of distributions encoding the nucleon structure

TMDs: Fraction of longitudinal momentum x et transverse momentum k

GPDs: Fraction of longitudinal momentum x et transverse position b

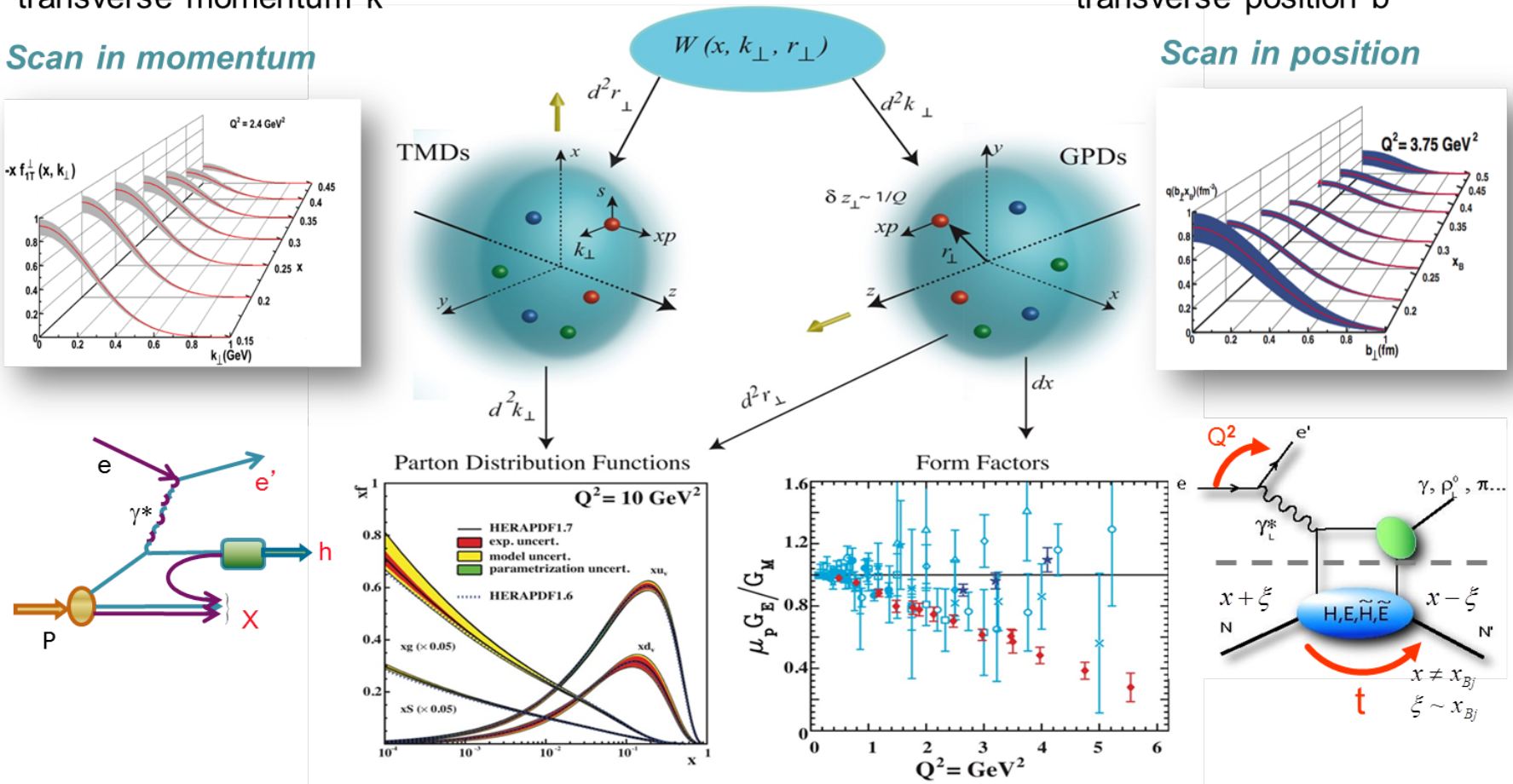

The deep exclusive processes

By measuring the cross section of deep exclusive processes, we get insights about the GPDs.

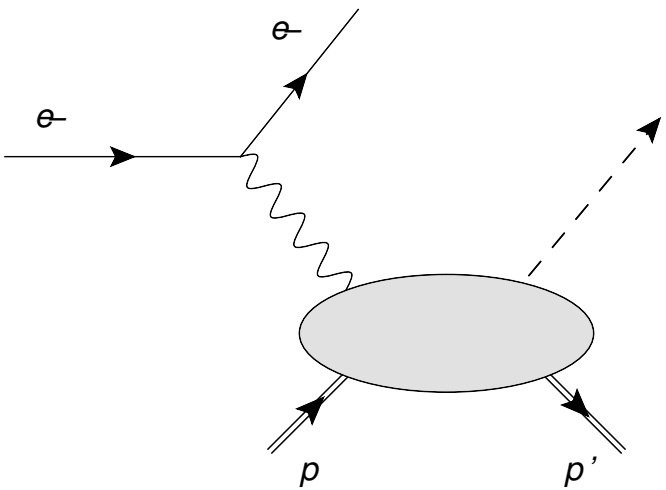

1. The electron interacts with the proton by exchanging a hard virtual photon.
2. The proton emits a particle (γ, π^0, ρ,...)

The link between these diagrams and the GPDs is guaranted by the factorization.

Factorization and GPDs

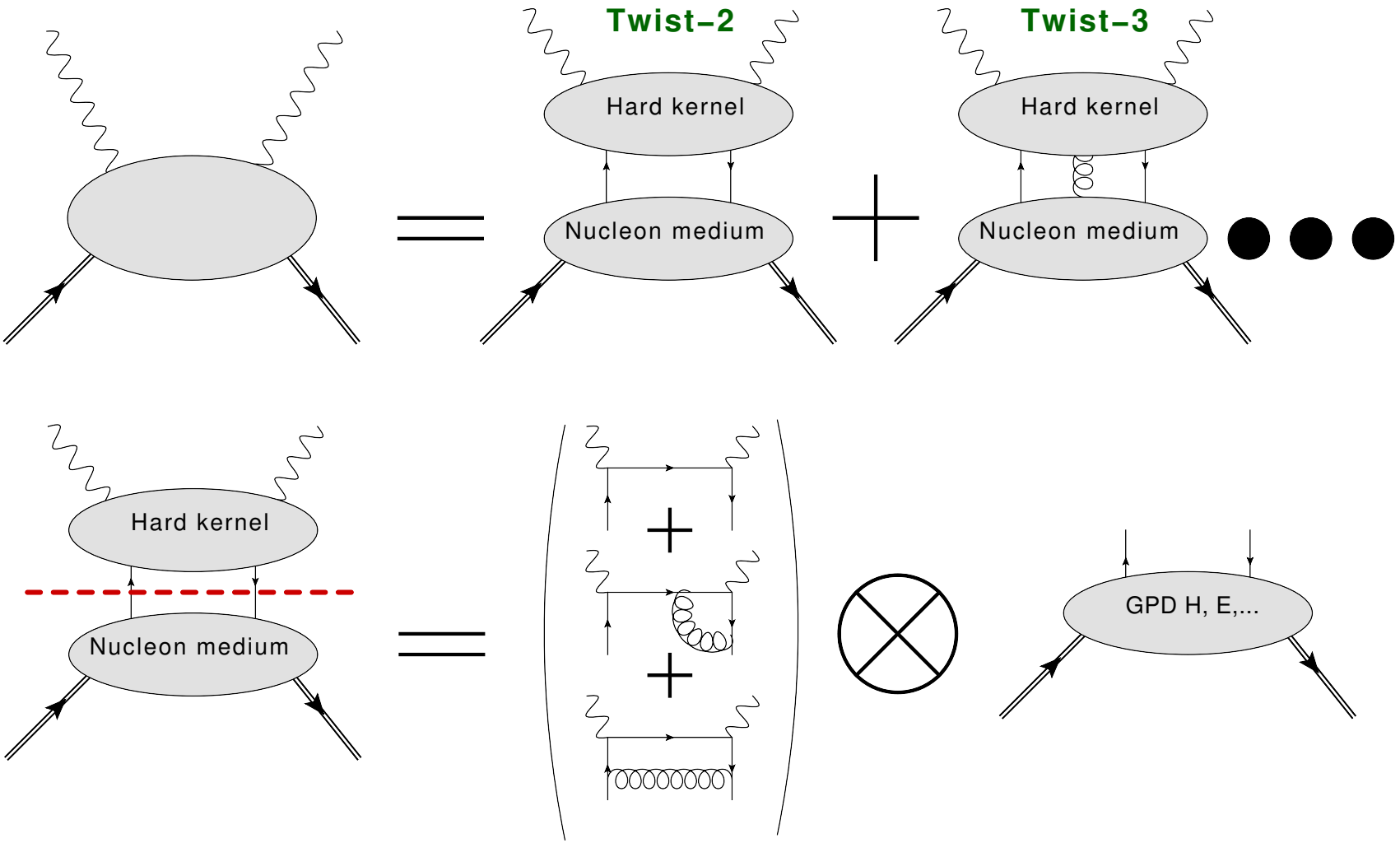

The amplitudes at twist-$(n+1)$ are suppressed by a factor $\frac{1}{Q}$ with respect to the twist-n amplitudes, with Q the virtuality of the photon.

DVCS and GPDs

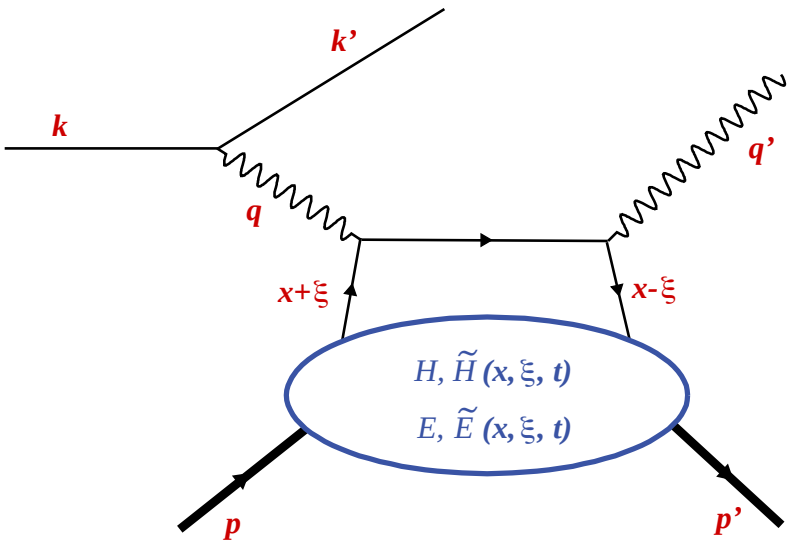

- $Q^2 = -q^2 = -(k - k')^2$.
- $x_B = \frac{Q^2}{2p \cdot q}$
- x longitudinal momentum fraction carried by the active quark.
- $\xi \sim \frac{x_B}{2 - x_B}$ the longitudinal momentum transfer.
- $t = (p - p')^2$ squared momentum transfer to the nucleon.

The GPDs enter the DVCS amplitude through a complex integral. This integral is called a *Compton form factor* (CFF).

$$\mathcal{H}_{++}(\xi, t) = \int_{-1}^{1} H(x, \xi, t) \left(\frac{1}{\xi - x - i\epsilon} - \frac{1}{\xi + x - i\epsilon} \right) dx \ .$$

The twist is also a story of polarization f the virtual photon!

Helicity amplitude and twist

The helicity amplitude $\mathcal{A}_{\mu+}$ is a linear combination of $\mathcal{H}_{\mu+}, \mathcal{E}_{\mu+}, \widetilde{\mathcal{H}}_{\mu+}, \widetilde{\mathcal{E}}_{\mu+}$, where μ stands for the helicity of the virtual photon.

- $\mathcal{A}_{++}$ which is leading-twist (twist-2).
- $\mathcal{A}_{-+}$ which is twist-4 at leading-order, or twist-2 if we have gluons.
- $\mathcal{A}_{0+}$,contribution from longitudinal polarization, which is twist-3.

Going to the cross section, you will have four terms arising from the previous amplitudes:

- The transverse term is σ_T which is the sum of $|\mathcal{A}_{++}|^2$ and $|\mathcal{A}_{-+}|^2$.
- The longitudinal term σ_L which is $|\mathcal{A}_{0+}|^2$.
- The interference term σ_{TL} which is an interference term obtained from $\mathcal{A}_{++} \times \mathcal{A}_{0+}$ and $\mathcal{A}_{++} \times \mathcal{A}_{0+}$.
- The interference term σ_{TT} which is an interference term obtained from $\mathcal{A}_{++} \times \mathcal{A}_{-+}$.

σ_T, σ_L,... and ϕ-dependence of the cross sections

The cross section of deep exclusive processes can be written under a common form:

$$\frac{d^4\sigma}{dtd\phi dQ^2 dx_B} = \frac{1}{2\pi}\Gamma_{\gamma^*}(Q^2, x_B, E_e)\Big[\frac{d\sigma_T}{dt} + \epsilon\frac{d\sigma_L}{dt} + \sqrt{2\epsilon(1+\epsilon)}\frac{d\sigma_{TL}}{dt}cos(\phi) + \epsilon\frac{d\sigma_{TT}}{dt}cos(2\phi)\Big],$$

For pseudo-scalar meson, the longitudinal response is the leading-twist one and the transverse one is higher-twist. For DVCS, it is the opposite.

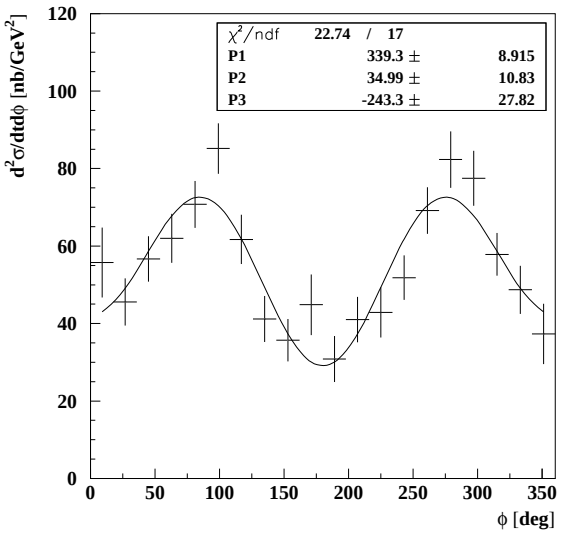

$ep \to ep\pi^0$ on the left: Striking evidence of higher-twist contributions because of ϕ-modulation.

For DVCS, it is more complicated.
I. Bedlinskiy *et al.* (CLAS collaboration), PhysRevC.90.025205 (2014)

Photon electroproduction and GPDs (PART I)

We use leptons beam to generate the γ^* in the initial state... not without consequences.
Indeed, experimentally we measure the cross section of the process $ep \to ep\gamma$ and not strictly $\gamma^* p \to \gamma p$.
Second level of interference with Bethe-Heitler making complicated the straightforward conclusion from ϕ-dependence

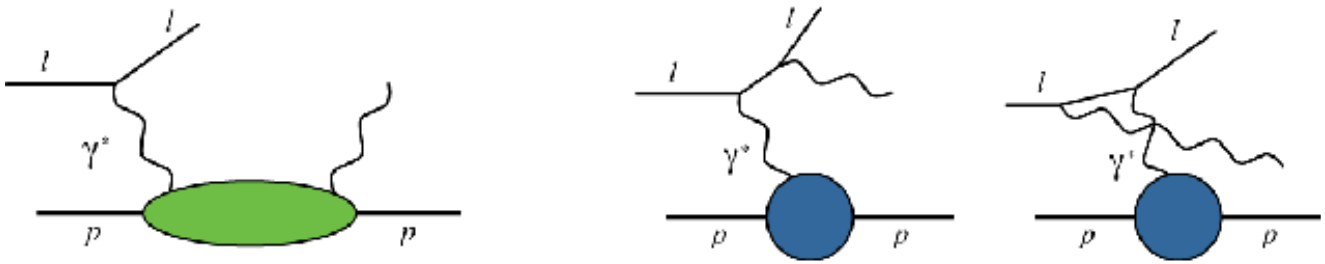

DVCS Bethe-Heitler

$$\frac{d^4\sigma(\lambda,\pm e)}{dQ^2 dx_B dt d\phi} = \frac{d^2\sigma_0}{dQ^2 dx_B}\frac{2\pi}{e^6} \times \left[\left|\mathcal{T}^{BH}\right|^2 + \left|\mathcal{T}^{DVCS}\right|^2 \mp \mathcal{I}\right] ,$$

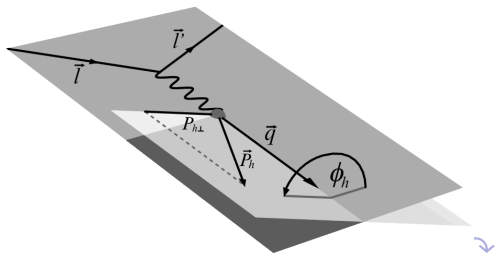

First DVCS experiment in Hall A in 2004

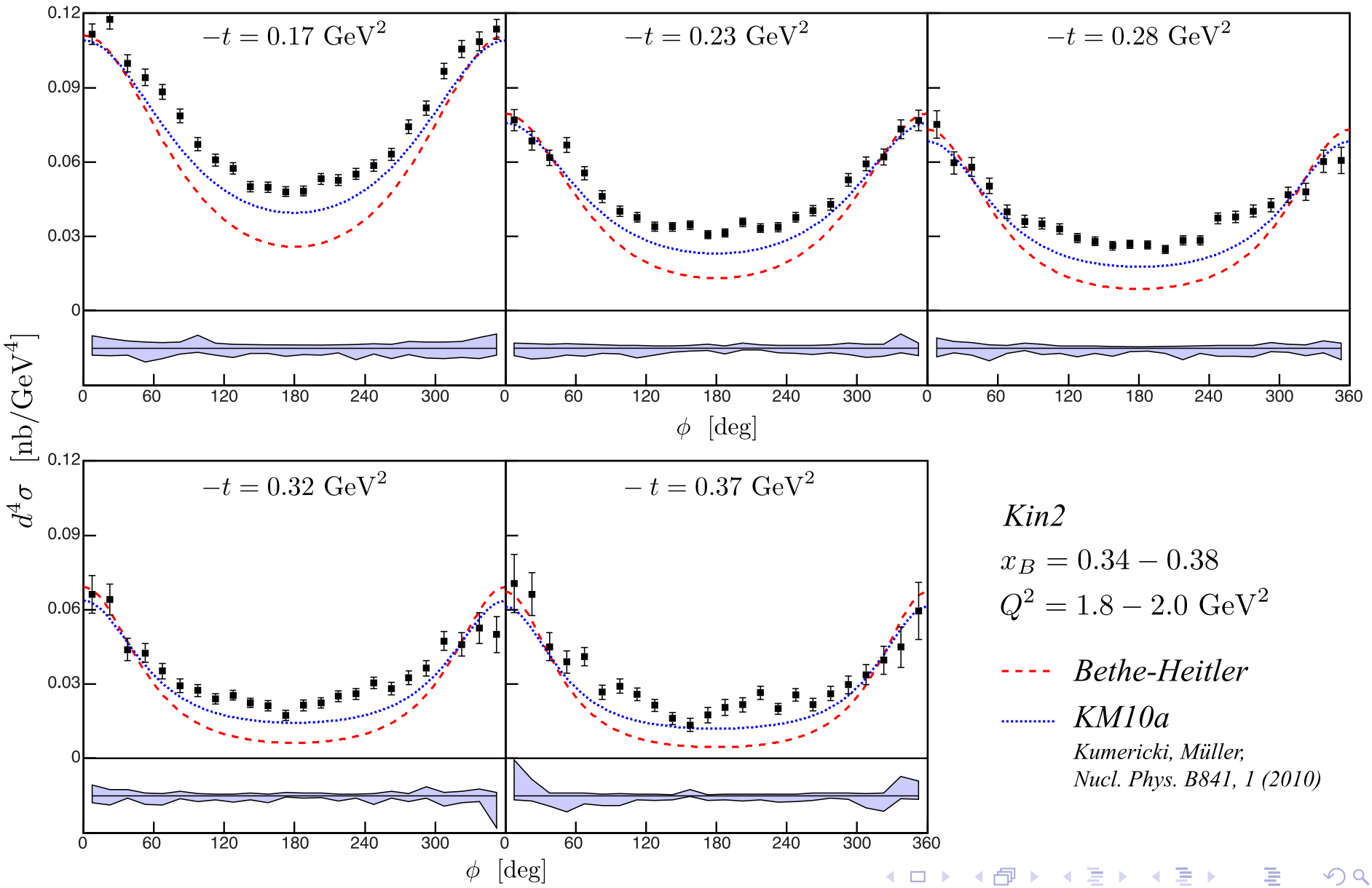

Kin2

$x_B = 0.34 - 0.38$

$Q^2 = 1.8 - 2.0$ GeV^2

Bethe-Heitler

KM10a

Kumericki, Müller, Nucl. Phys. B841, 1 (2010)

A parameterization of cross section

The CFFs are encapsulated in the harmonics c_n and s_n of both DVCS and interference. In the leading twist approximation for unpolarized target:

$$c_0^{DVCS} \propto \mathcal{C}^{DVCS}(\mathcal{F}_{++}, \mathcal{F}_{++}^*) = 4(1-x_B)\mathcal{H}_{++}\mathcal{H}_{++}^* + \cdots \quad (1)$$

$$c_1^{\mathcal{I}} \propto Re\ \mathcal{C}^{\mathcal{I}}(\mathcal{F}_{++}) = F_1\ Re\mathcal{H}_{++} + \xi(F_1+F_2)\ Re\widetilde{\mathcal{H}}_{++} - \frac{t}{4M^2}F_2\ Re\mathcal{E}_{++}\,,$$

$$s_1^{\mathcal{I}} \propto Im\ \mathcal{C}^{\mathcal{I}}(\mathcal{F}_{++}) = F_1\ Im\mathcal{H}_{++} + \xi(F_1+F_2)\ Im\widetilde{\mathcal{H}}_{++} - \frac{t}{4M^2}F_2\ Im\mathcal{E}_{++}\,,$$

We gain access to real and imaginary part of CFFs, but lose the direct access to DVCS.

BH and DVCS have different beam energy dependence $\rightarrow$ Rosenbluth separation to separate them all.

Setting	E (GeV)	Q^2 (GeV^2)	x_B	W (GeV)
2010-Kin1	(3.355 ; 5.55)	1.5	0.36	1.9
2010-Kin2	(4.455 ; 5.55)	1.75	0.36	2
2010-Kin3	(4.455 ; 5.55)	2	0.36	2.1

Mueller D., Belitsky A.V., Phys.Rev.D.82 (2010)

The experimental setup

We want to study $ep \rightarrow ep\gamma$:

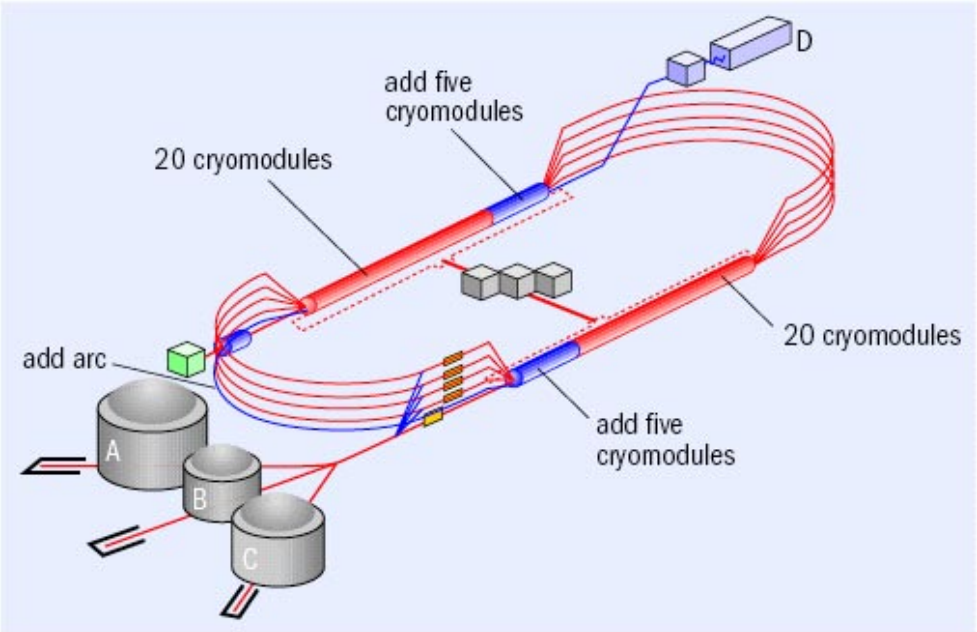

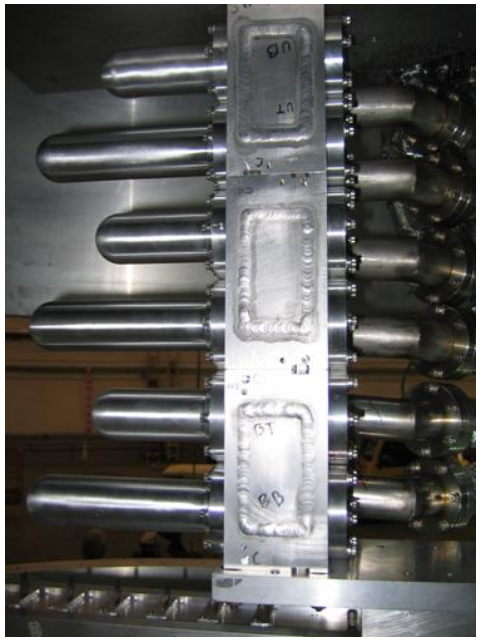

The accelerator provided:

- 80% longitudinally polarized electron beam on a 15 cm-long LH_2 target,
- with a maximal beam current of 200 μA (I<4 μA),
- up to 6 GeV (now 12 GeV).

The experimental setup

We want to study $ep \rightarrow ep\gamma$:

In the Hall A,

- The scattered electron is detected by a High Resolution Spectrometer (HRS): We measure accurately x_B and Q^2.
- The photon is detected by an electromagnetic calorimeter: The 4-momenta of the scattered electron and the photon gives t and ϕ.

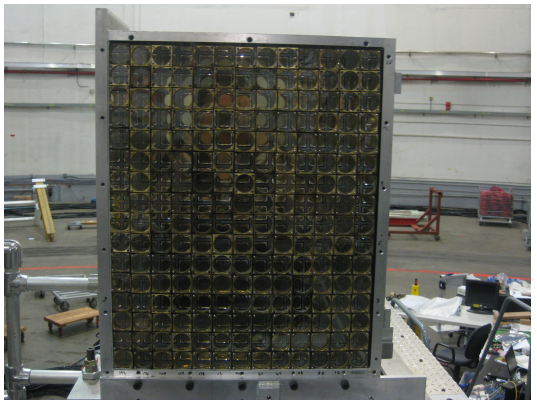

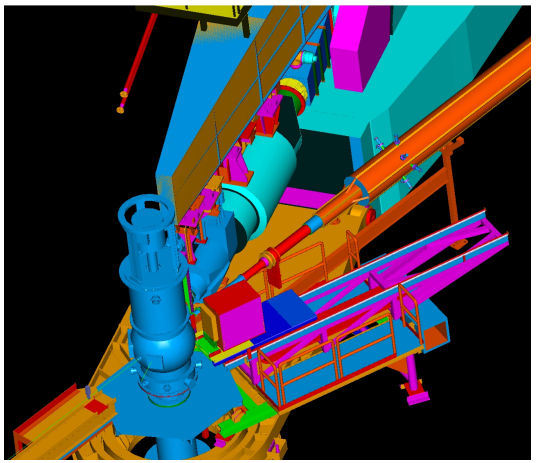

$N_{M_X^2 < M_{cut}^2} = N_{ep \to ep\gamma} + N_{acc} + N_{\pi^0 - 1\gamma} + N_{SIDIS}$

- N_{SIDIS} cannot be subtracted and we need to cut low enough in missing mass to have:

$$N_{SIDIS} << N_{ep \to e\gamma p}$$

- The fraction of exclusive events lost with the cut is corrected through the Monte-Carlo simulation.

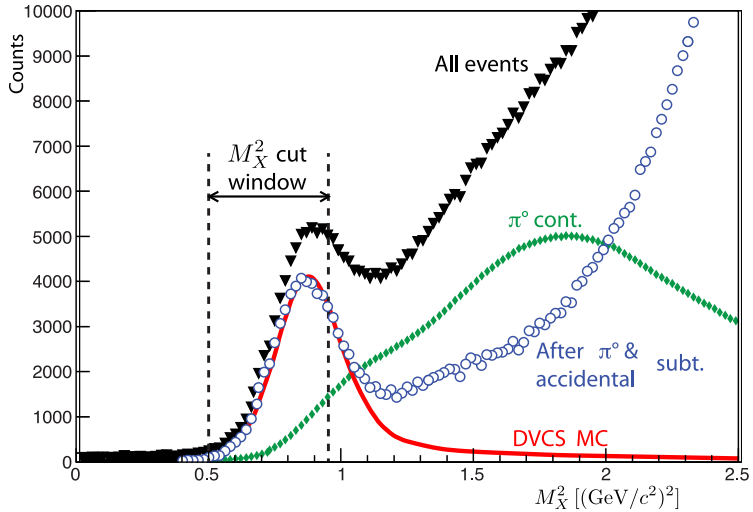

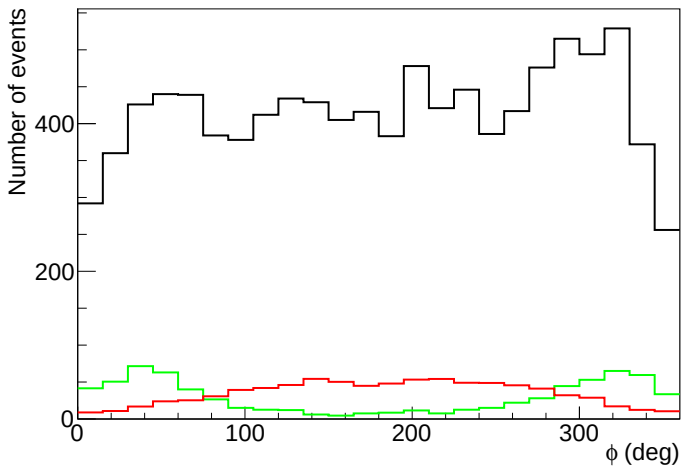

The calorimeter resolution: A crucial effect

The events of a specific t and ϕ bins are located in a specific area of the calorimeter.

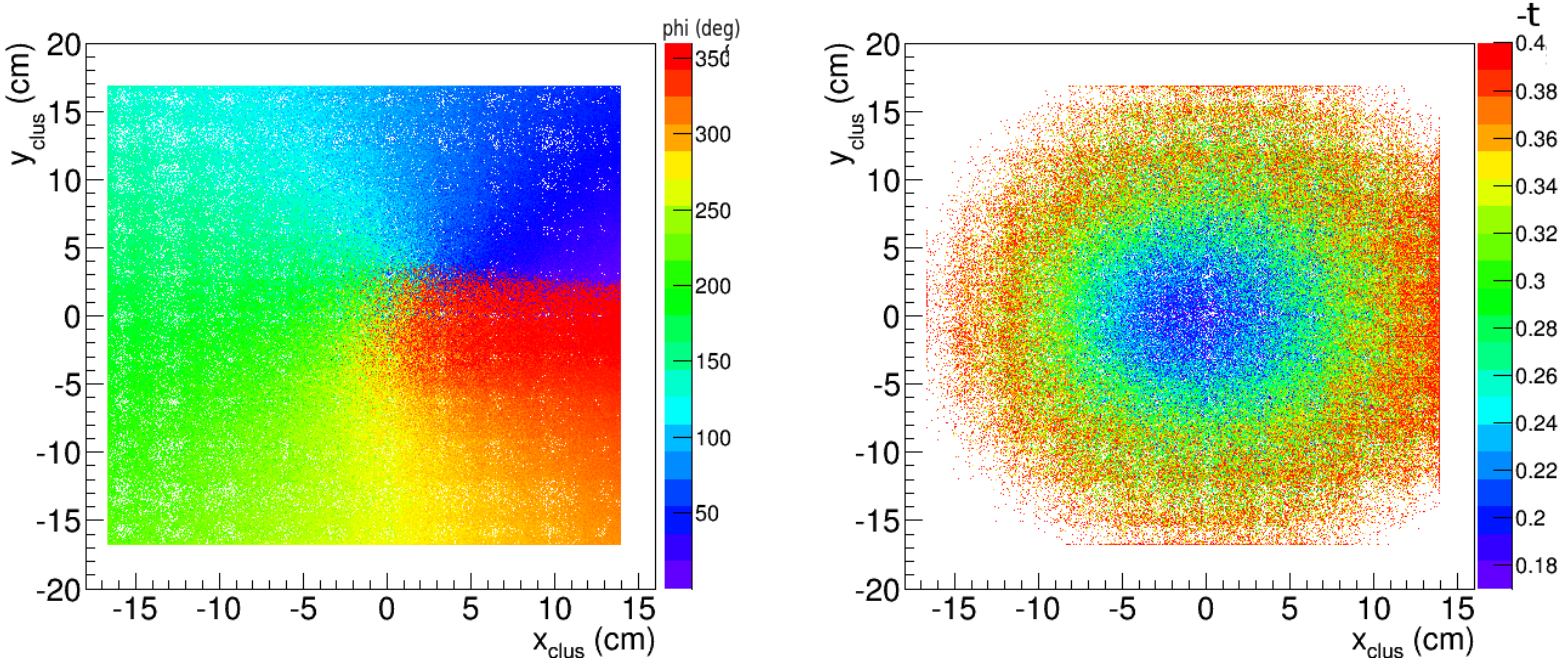

Figure: Left: ϕ-distribution of the events as a function of the photon position in the calorimeter. Right: t-distribution of the events as a function of the photon position in the calorimeter.

The calorimeter resolution: A crucial effect

From one edge of the calorimeter to the other, the energy resolution is not the same ($\phi = 0°$ in red et $\phi = 180°$ in blue).

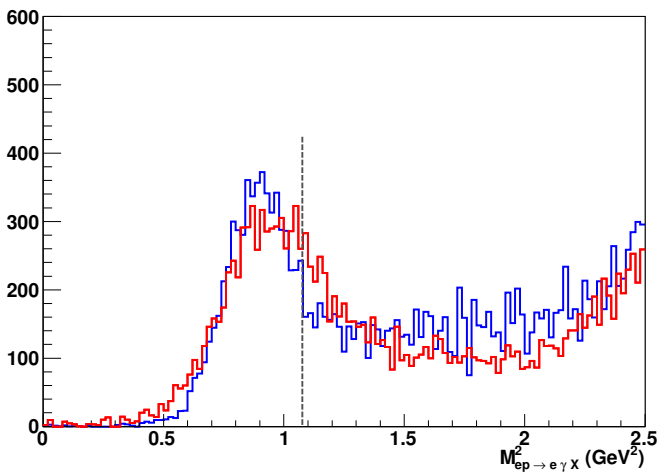

	μ (GeV^2)	σ (GeV^2)
Beam-side (red)	0.964	0.213
180°-side (blue)	0.902	0.144
sum (red+blue)	0.914	0.167

Table: Mean value μ and standard deviation σ of a gaussian fitted on the squared missing mass distributions.

Assuming a uniform resolution and calibration, we would have induced a -15% shift of the cross section at 0° and +5% at 180°.

The calorimeter resolution: A crucial effect

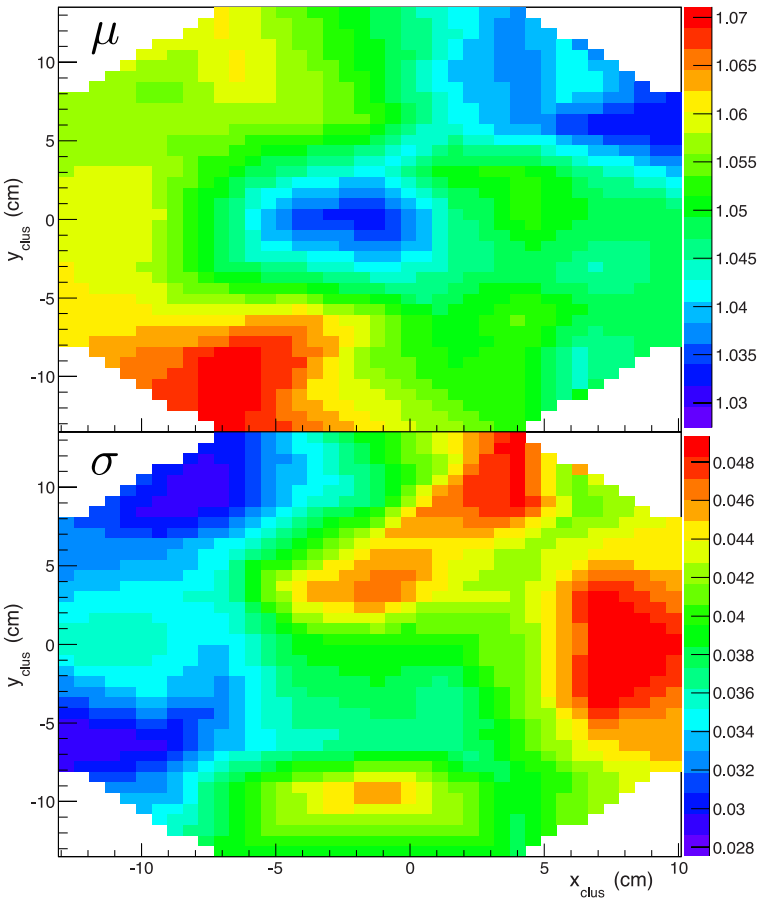

I have developed a calibration/smearing/fit method for the Monte-Carlo calorimeter

$$\begin{pmatrix} q_x \\ q_y \\ q_z \\ E \end{pmatrix} \longmapsto gaus(\mu, \sigma) \times \begin{pmatrix} q_x \\ q_y \\ q_z \\ E \end{pmatrix},$$

which reproduces locally the resolution.

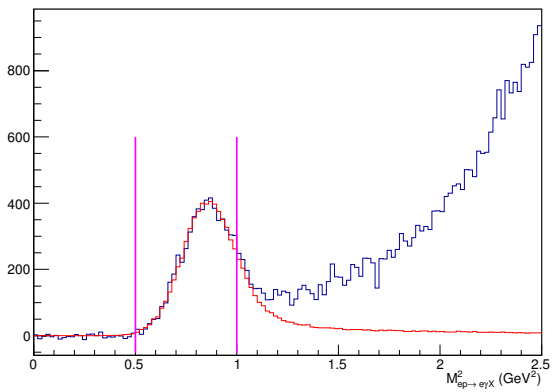

Before final results, let's compare 2004-2010

While analyzing the 2010 data, a new fit including the previous results has been produced.

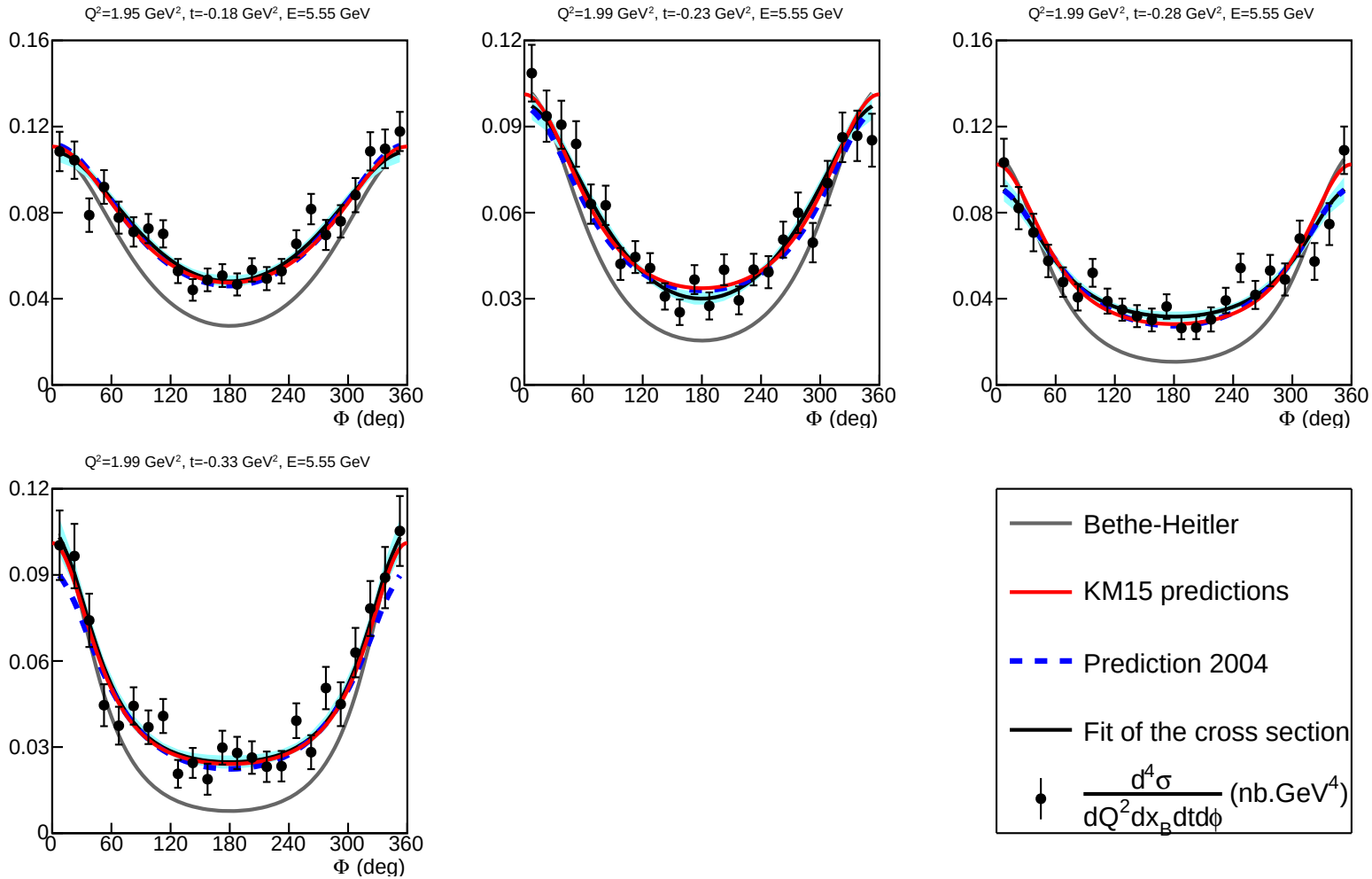

A fit of CFFs including kinematical power corrections

Kinematical power corrections sizeable and changing the beam-energy dependences!

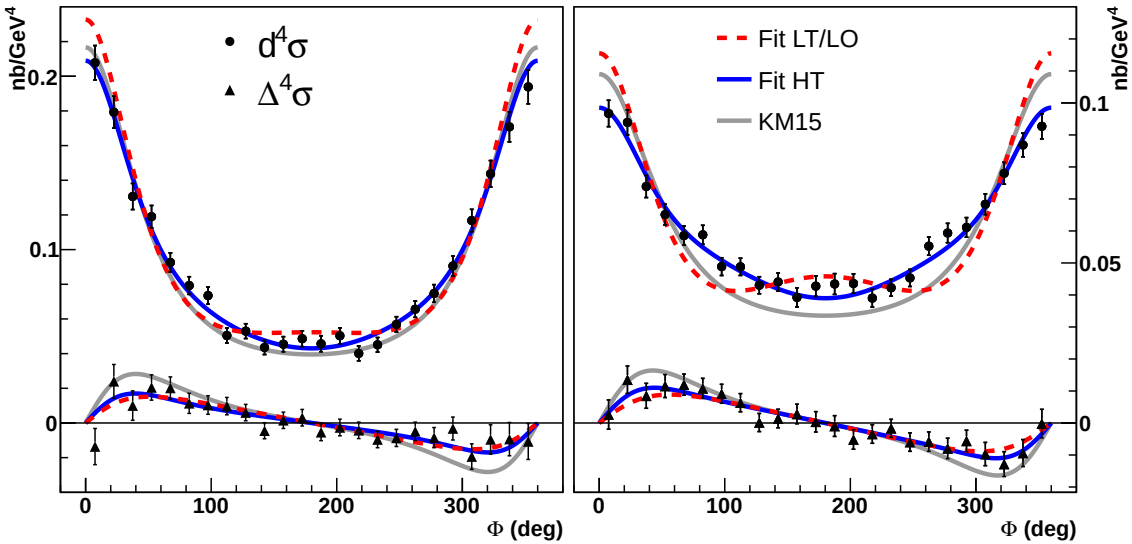

Figure: Q^2=1.75 GeV^2, -t=0.3 GeV^2. E=4.445 GeV (left) and E=5.55 GeV (right)

- LT/LO: $\mathbb{H}_{++}, \mathbb{E}_{++}, \tilde{\mathbb{H}}_{++}, \tilde{\mathbb{E}}_{++}$.
- HT: $\mathbb{H}_{++}, \tilde{\mathbb{H}}_{++}, \mathbb{H}_{0+}, \tilde{\mathbb{H}}_{0+}$.
- NLO: $\mathbb{H}_{++}, \tilde{\mathbb{H}}_{++}, \mathbb{H}_{-+}, \tilde{\mathbb{H}}_{-+}$.

Equally good fit between the HT and NLO scenario.

M. Defurne *et al.*, Hall A collaboration, Nature Communications 8, 1408 (2017)

Separation of DVCS and interference

Despite an equally good fit, slight differences appear when separating the interference and DVCS term.
Non-flat DVCS^2!!!

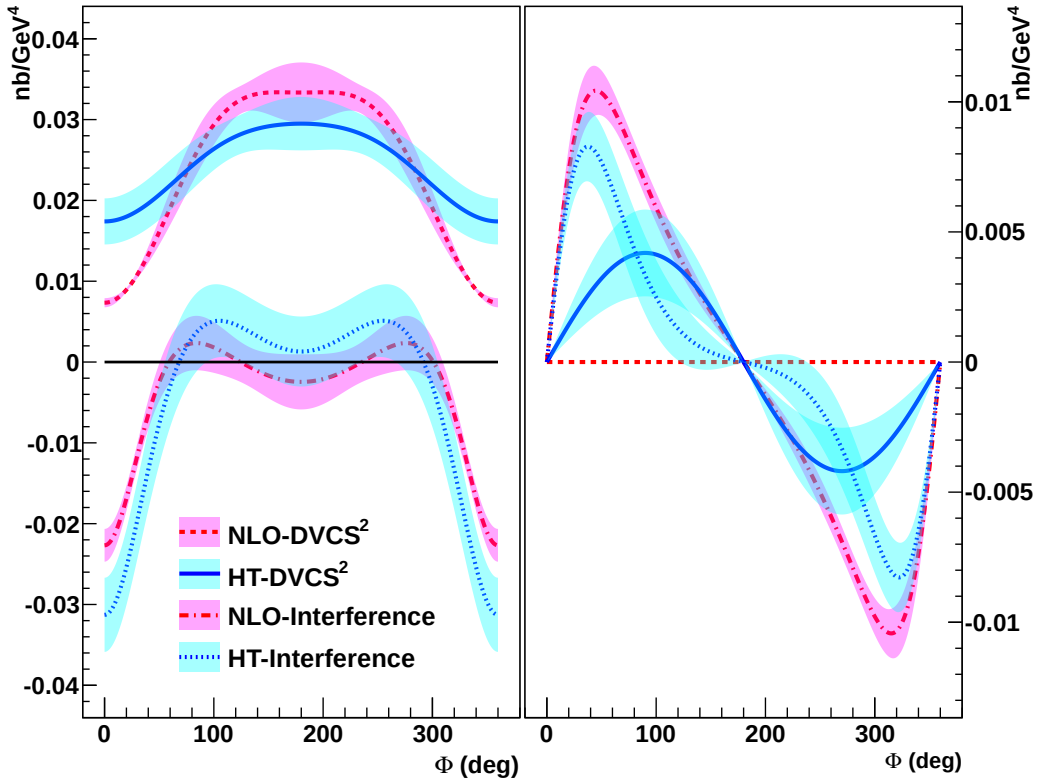

In the HT scenario, the beam helicity dependent cross section is not a pure interference term, as it is usually assumed in most phenomenological analyses. M. Defurne *et al.*, Hall A collaboration, Nature Communications 8, 1408 (2017)

Conclusion

- Kinematical power corrections have be taken into account for the first time in phenomenological analysis.
- First proof of higher-twist and/or Next-to-Leading order contributions in DVCS for JLab-6GeV data.
- At 11 GeV, Bethe-Heitler can be dramatically reduced at some Q^2 and x_B values.
- People start discussing about positron beam (see my talk at JPos workshop!).

A rich program concerning DVCS at JLab with two Rosenbluth separation experiments in Hall B and Hall C

And cannot wait to see the first results from Hall A at 12 GeV.

Thank you!

The experimental setup

We want to study $ep \rightarrow ep\gamma$:

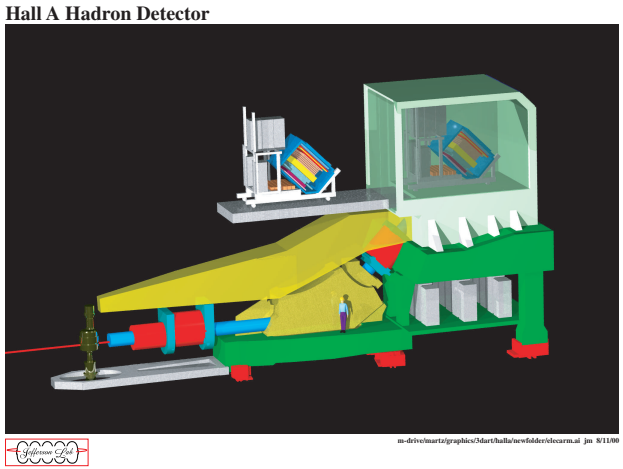

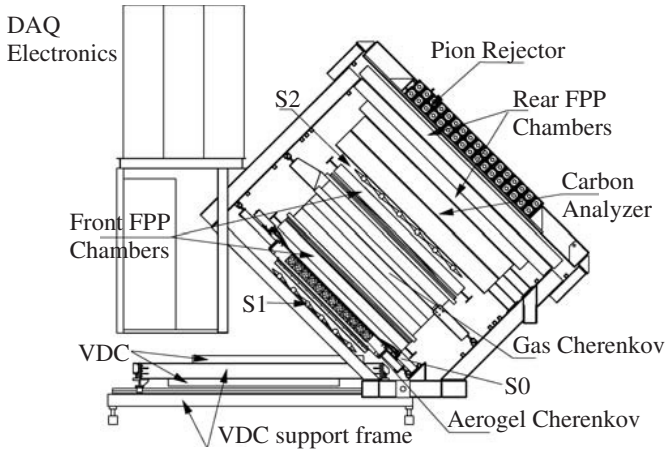

The High Resolution spectrometer detects and characterizes the scattered electron:
$\frac{\delta p}{p} \simeq 2.10^{-4}$ and solid angle $\simeq 6$ msr.

It allows an accurate measurement of Q^2 and x_B.

Scintillators and Čerenkov detector were part of the trigger.

$N_{M_X^2 < M_{cut}^2} = N_{ep \to ep\gamma} + N_{acc} + N_{\pi^0 - 1\gamma} + N_{SIDIS}$

[noframenumbering]

Accidentals are time-independent.

Estimated by studying events outside of the coincidence window.

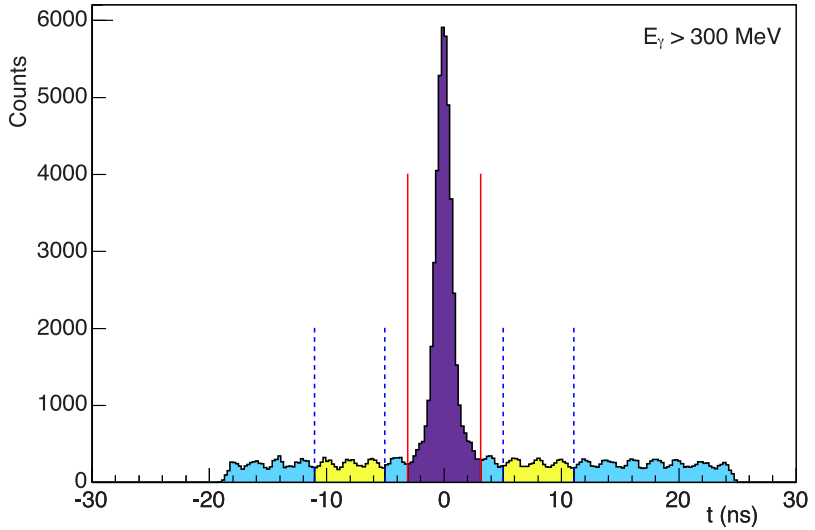

Accidentals are mostly located around $\phi = 0°$. We require a missing mass higher than 0.5 GeV^2 to reduce the statistical uncertainty from the subtraction.

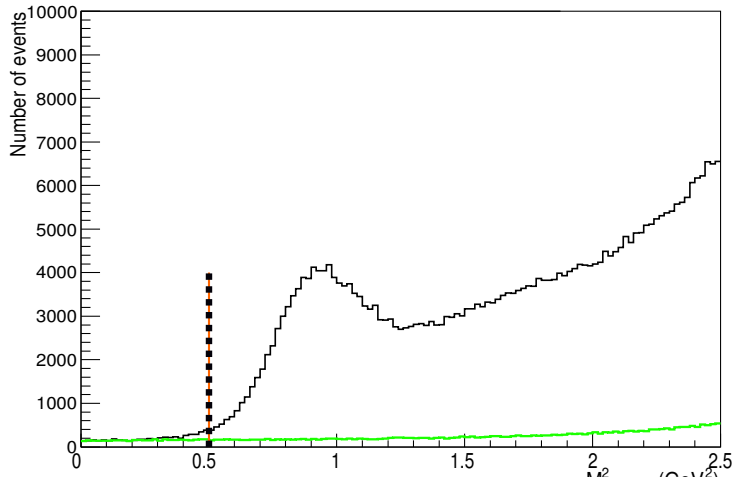

$N_{M_X^2 < M_{cut}^2} = N_{ep \to ep\gamma} + N_{acc} + N_{\pi^0 - 1\gamma} + N_{SIDIS}$

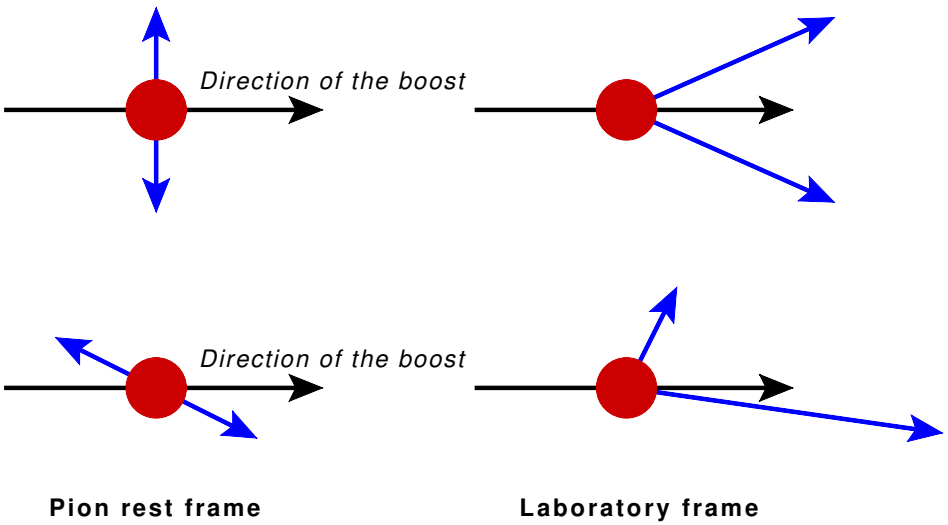

The kinetic energy of the π^0 is shared between the two photons depending on their direction with respect to the π^0 momentum.

We just need to evaluate the phase space of decay contributing to the contamination.

Principle: For each detected π^0, generate a large number of decays to estimate the contamination.

- Detect the two photons.
- Detect only one of the two photons.
- Considered as exclusive photon events.

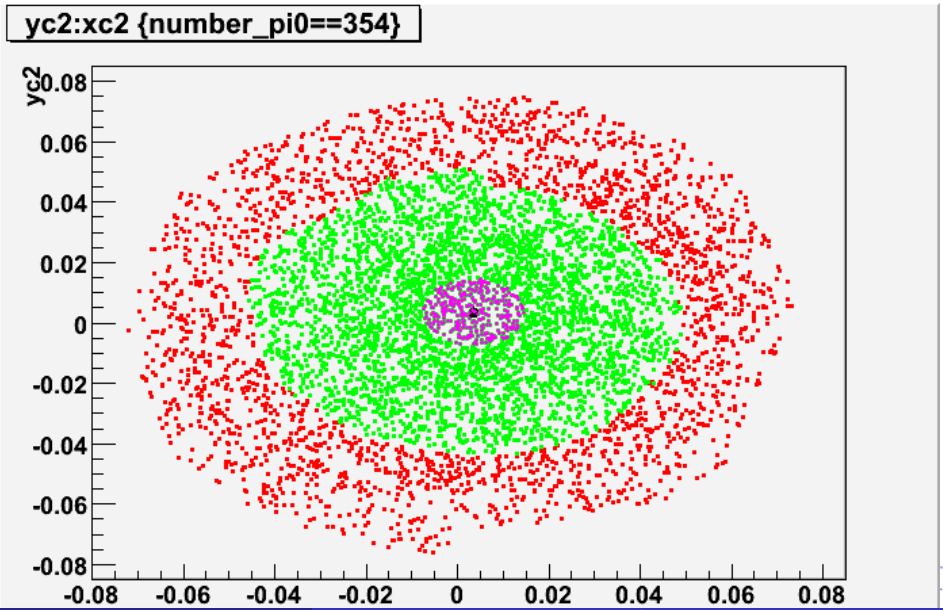

$N_{M_X^2 < M_{cut}^2} = N_{ep \to ep\gamma} + N_{acc} + N_{\pi^0 - 1\gamma} + N_{SIDIS}$

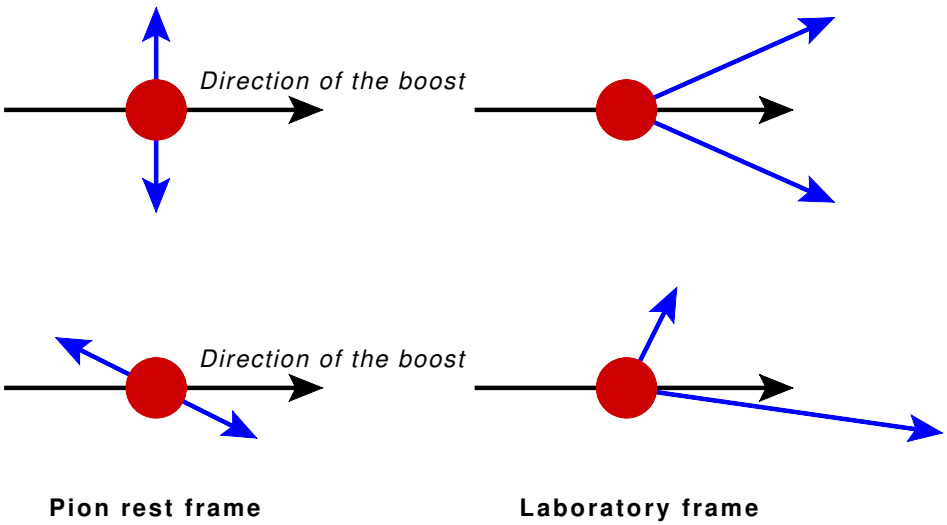

The kinetic energy of the π^0 is shared between the two photons depending on their direction with respect to the π^0 momentum.

We just need to evaluate the phase space of decay contributing to the contamination.

- Advantage: No need for a parameterization of π^0 cross section.
- Drawback: Depends on the ability to detect the 2 photons.

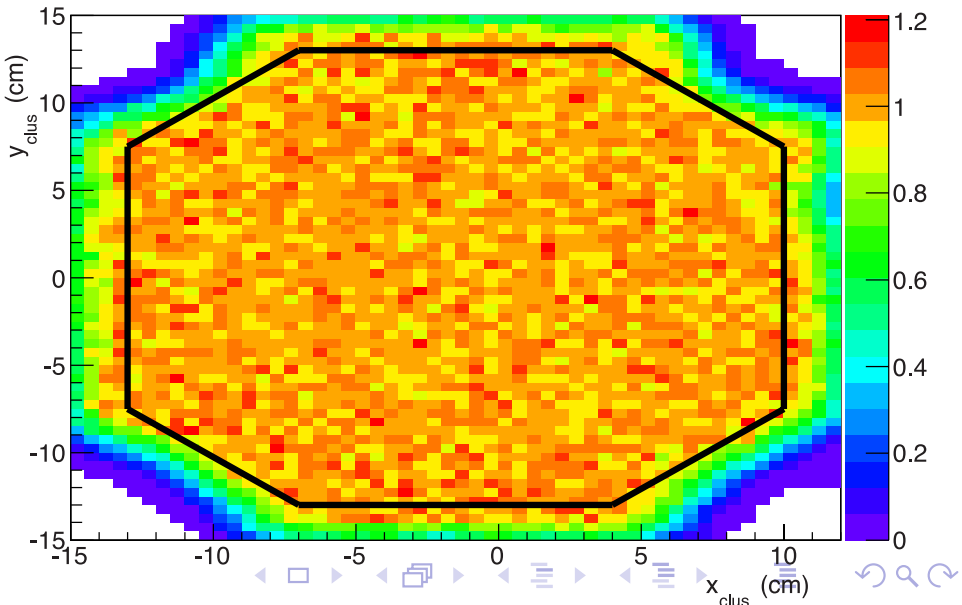

Where do the kinematical power corrections come from?

The helicity decomposition is frame-dependent. Braun et al. chose a frame which makes easier the inclusion of kinematically suppressed terms (in t/Q^2 or M^2/Q^2). In the BMP formalism, the cross section is parametrized by a set of CFFs:

$$\mathbb{F}_{\mu\nu} \in \left\{ \mathbb{H}_{\mu\nu}, \mathbb{E}_{\mu\nu}, \tilde{\mathbb{H}}_{\mu\nu}, \tilde{\mathbb{E}}_{\mu\nu} \right\} \tag{2}$$

where μ (ν) is the helicity of the virtual (real) photon. Therefore we can distinguish three cases:

- $\mathbb{F}_{++}$ are the *helicity-conserved CFFs*. They are twist-2 CFFs.
- $\mathbb{F}_{0+}$ are the *longitudinal-to-transverse helicity flip CFFs*. They are *twist-3* CFFs.
- $\mathbb{F}_{-+}$ are the *transverse-to-transverse helicity flip CFFs*. At LO, these CFFs are *twist-4*. At NLO, these CFFs involves the gluon transversity GPDs.

BMP... BMJ... which difference?

But let's stay at leading-order. The BMP CFFs are not the same as the BMJ CFFs. The BMP CFFs are more complex terms. As an example, $\mathbb{H}_{++}$, we have:

$$\mathcal{H}_{++} = T_0 \otimes H \,, \tag{3}$$

$$\mathbb{H}_{++} = T_0 \otimes H + \frac{-t}{Q^2}\left[\frac{1}{2}T_0 - T_1 - 2\xi D_\xi T_2\right] \otimes H + \frac{2t}{Q^2}\xi^2 \partial_\xi T_2 \otimes (H+E) \,. \tag{4}$$

We can go from BMP to BMJ CFFs by making the following replacement:

$$\mathcal{F}_{++} = \mathbb{F}_{++} + \frac{\chi}{2}\left[\mathbb{F}_{++} + \mathbb{F}_{-+}\right] - \chi_0 \mathbb{F}_{0+} \,, \tag{5}$$

$$\mathcal{F}_{-+} = \mathbb{F}_{-+} + \frac{\chi}{2}\left[\mathbb{F}_{++} + \mathbb{F}_{-+}\right] - \chi_0 \mathbb{F}_{0+} \,, \tag{6}$$

$$\mathcal{F}_{0+} = -(1+\chi)\mathbb{F}_{0+} + \chi_0\left[\mathbb{F}_{++} + \mathbb{F}_{-+}\right] \,, \tag{7}$$

with: $\chi_0 \propto \sqrt{t'}/Q$ and $\chi \propto t'/Q^2$. The leading-twist assumption gives different results between BMP and BMJ.

Differences in the LT-LO assumption: BMJ

Assuming leading-twist and LO in BMJ, we have $\mathcal{F}_{-+} = 0$ and $\mathcal{F}_{0+} = 0$. It is important when regarding the DVCS amplitude. We have:

$$c_{0,\mathrm{unp}}^{\mathrm{VCS}} = 2\frac{2 - 2y + y^2 + \frac{\epsilon^2}{2}y^2}{1+\epsilon^2}\,\mathcal{C}_{\mathrm{unp}}^{\mathrm{VCS}}(\mathcal{F}_{\pm+}, \mathcal{F}_{\pm+}^*) + 8\frac{1 - y - \frac{\epsilon^2}{4}y^2}{1+\epsilon^2}\,\mathcal{C}_{\mathrm{unp}}^{\mathrm{VCS}}(\mathcal{F}_{0+}, \mathcal{F}_{0+}^*)\,, \tag{8}$$

$$\begin{Bmatrix} c_{1,\mathrm{unp}}^{\mathrm{VCS}} \\ s_{1,\mathrm{unp}}^{\mathrm{VCS}} \end{Bmatrix} = \frac{4\sqrt{2}\sqrt{1 - y - \frac{\epsilon^2}{4}y^2}}{1+\epsilon^2} \begin{Bmatrix} 2 - y \\ -\lambda y\sqrt{1+\epsilon^2} \end{Bmatrix} \begin{Bmatrix} \Re\mathrm{e} \\ \Im\mathrm{m} \end{Bmatrix} \mathcal{C}_{\mathrm{unp}}^{\mathrm{VCS}}\left(\mathcal{F}_{0+} \middle| \mathcal{F}_{++}^*, \mathcal{F}_{-+}^*\right), \tag{9}$$

$$c_{2,\mathrm{unp}}^{\mathrm{VCS}} = 8\frac{1 - y - \frac{\epsilon^2}{4}y^2}{1+\epsilon^2}\,\Re\mathrm{e}\,\mathcal{C}_{\mathrm{unp}}^{\mathrm{VCS}}\left(\mathcal{F}_{-+}, \mathcal{F}_{++}^*\right). \tag{10}$$

which reduces to:

$$c_{0,\mathrm{unp}}^{\mathrm{VCS}} = 2\frac{2 - 2y + y^2 + \frac{\epsilon^2}{2}y^2}{1+\epsilon^2}\,\mathcal{C}_{\mathrm{unp}}^{\mathrm{VCS}}(\mathcal{F}_{++}, \mathcal{F}_{++}^*) \tag{11}$$

The DVCS amplitude is ϕ-**independent** with a **single** beam-energy dependence.

Differences in the LT-LO assumption: BMP

Assuming leading-twist and LO in BMP, we have $\mathbb{F}_{-+} = 0$ and $\mathbb{F}_{0+} = 0$.

$$\mathcal{F}_{++} = \left(1 + \tfrac{\chi}{2}\right) \mathbb{F}_{++} \,, \tag{12}$$

$$\mathcal{F}_{-+} = \tfrac{\chi}{2} \mathbb{F}_{++} \,, \tag{13}$$

$$\mathcal{F}_{0+} = \chi_0 \mathbb{F}_{++} \,, \tag{14}$$

It is important when regarding the DVCS amplitude.

$$c_{0,\mathrm{unp}}^{\mathrm{VCS}} = 2\frac{2 - 2y + y^2 + \frac{\epsilon^2}{2} y^2}{1 + \epsilon^2} \mathcal{C}_{\mathrm{unp}}^{\mathrm{VCS}}(\mathcal{F}_{\pm+}, \mathcal{F}_{\pm+}^*) + 8\frac{1 - y - \frac{\epsilon^2}{4} y^2}{1 + \epsilon^2} \mathcal{C}_{\mathrm{unp}}^{\mathrm{VCS}}(\mathcal{F}_{0+}, \mathcal{F}_{0+}^*) \,, \tag{15}$$

$$\begin{Bmatrix} c_{1,\mathrm{unp}}^{\mathrm{VCS}} \\ s_{1,\mathrm{unp}}^{\mathrm{VCS}} \end{Bmatrix} = \frac{4\sqrt{2}\sqrt{1 - y - \frac{\epsilon^2}{4} y^2}}{1 + \epsilon^2} \begin{Bmatrix} 2 - y \\ -\lambda y \sqrt{1 + \epsilon^2} \end{Bmatrix} \begin{Bmatrix} \Re\mathrm{e} \\ \Im\mathrm{m} \end{Bmatrix} \mathcal{C}_{\mathrm{unp}}^{\mathrm{VCS}} \left(\mathcal{F}_{0+} \middle| \mathcal{F}_{++}^*, \mathcal{F}_{-+}^*\right) , \tag{16}$$

$$c_{2,\mathrm{unp}}^{\mathrm{VCS}} = 8\frac{1 - y - \frac{\epsilon^2}{4} y^2}{1 + \epsilon^2} \Re\mathrm{e}\, \mathcal{C}_{\mathrm{unp}}^{\mathrm{VCS}} \left(\mathcal{F}_{-+}, \mathcal{F}_{++}^*\right) . \tag{17}$$

The DVCS amplitude is **no longer** ϕ-independent with **multiple** beam-energy dependences.

A complicated Rosenbluth separation

By changing the beam energy, we also change the polarization of the virtual photon.

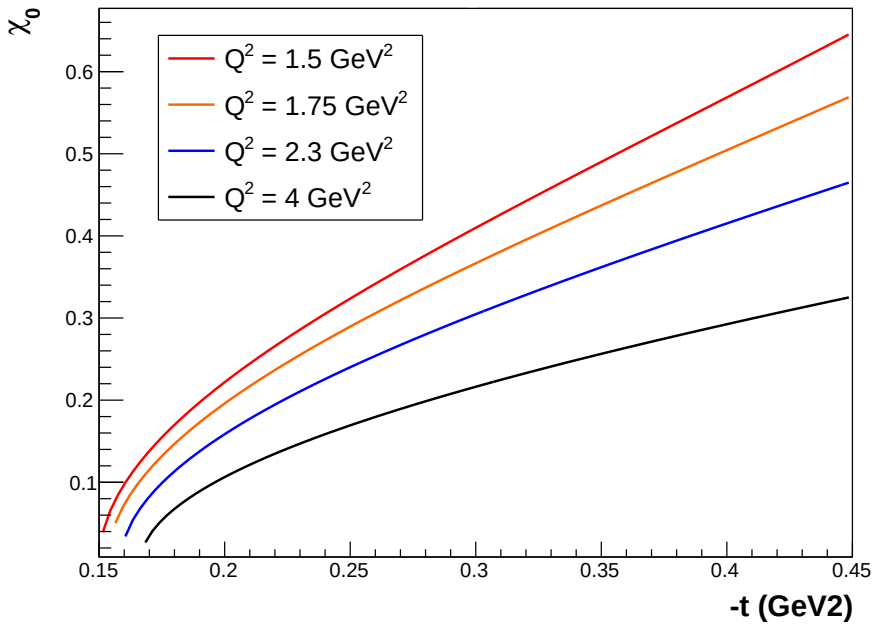

We must take them into account. Let's fit the real and imaginary parts of $\mathbb{H}_{++}\mathbb{E}_{++}\tilde{\mathbb{H}}_{++}\tilde{\mathbb{E}}_{++}$:

- simultaneously on unpolarized and polarized cross sections,
- simultaneously on the two beam energies,
- simultaneously for the three Q^2-values (but I neglect the Q-evolution),